Understanding of Leading-Edge Protection Performance Using Nano-Silicates for Modification

IOP Conf. Series: Journal of Physics: Conf. Series **1222** (2019) 012016 doi:10.1088/1742-6596/1222/1/012016

Understanding of Leading-Edge Protection Performance Using Nano-Silicates for Modification

I Ouachan[1*], M Kuball[2], D Liu[2], K Dyer[3], C Ward[1] and I Hamerton[1]

[1]Bristol Composites Institute (ACCIS), University of Bristol, Bristol, BS8 1TR, UK.
[2] H. H. Wills Physics Laboratory, University of Bristol, Bristol BS8 1TL, UK;
[3] Offshore Renewable Energy Catapult (ORE), Glasgow, G1 1RD, UK;
* Corresponding author (Imad.Ouachan@bristol.ac.uk)

Abstract. Leading edge erosion caused by raindrop impact is a key problem that needs to be overcome in the wind energy sector. Solutions up to date have not proved suitable, failing prematurely in their lifecycle at a cost to the wind industry. Failure mechanisms for rain erosion are not well understood, particularly the elastic and viscous polymer properties at the resulting high strain rates (10^6 - 10^9 Hz) of raindrop impacts. The effect of the inclusion of glycidyl polyhedral oligomeric silsesquioxane nanoparticles into a commercial polyurethane coating system was studied using nanoindentation and dynamic mechanical thermal analysis (DMTA). Results show that the inclusion of POSS improves damping, providing an alternative mechanism for energy dissipation without variation of T_g and minimal loss of stiffness. This presents a way of modifying current coating systems through the incorporation of POSS. Nanoindentation obtained previously unreported properties of the coating system (hardness, modulus and short-term recovery) and highlighted a correlation between loading rate and a reduction of short-term recovery. Nanoindentation was difficult for the modified leading-edge protection (LEP) samples as two phases were formed resulting in large standard deviations. DMTA results show modification of the LEP increases damping at lower temperature ranges introducing an additional mechanism of dissipating energy. Additionally, sweep data show an increase in elasticity at higher frequencies on the modified samples.

1. Introduction

Offshore wind turbine blades are expected to remain in operation with minimal maintenance for a service life of 25 years. However, it is estimated that up to £1.3 million is spent on each turbine during its lifetime due to leading edge erosion (LEE) from the impact of rain droplets with current coating systems [1]. Erosion can be reduced by limiting blade tip speeds (currently ~100 m/s), but with reduced noise restrictions offshore, the current trend is for increasing the blade length and tip speeds to maximise the potential of wind turbines in an already competitive energy market. LEE can be caused by rain, hail, sea spray, and other particulate debris such as sand, dependent on the operating environment. For offshore wind turbines liquid droplet impingement results in significant blade erosion which is detrimental to aerodynamic efficiency and, as a result, decreased energy capture. A recent campaign by Offshore Renewable Energy Catapult aimed to provide more representative results by measuring the effect of erosion on the annual energy production of operating offshore wind turbines [1]. It was found that an uplift in annual energy production between 1.5 % and 2 % can be achieved following the repair of moderate erosion. This is seen as a significant issue as it not only decreases energy capture over time but also requires regular inspections and sometimes substantial repair.

General current offshore solutions that are available include [2, 3]:

- gelcoats *e.g.* epoxy or polyester and form a chemical bond between the two during single cure;
- flexible coatings which are applied post moulding using rollers or spray equipment.
- rain erosion shields which are premade in controlled conditions and bonded to the blade.

Cortes *et al.* reported that lower modulus flexible coatings are better against rain erosion in comparison to stiffer gelcoat types [3]. This is thought to be due to the reduction of stress at the impact surface and damping the peak value of the initial stress wave, ensuring rapid material recovery and optimised energy dissipation. Elastomeric and ductile polymer coatings generally undergo ductile erosion behaviour, dependent on the rain impact conditions, with elastomers showing a much lower weight loss [4]. This has been attributed to how the materials removal occurs – tearing and fatigue for rubbers, cutting and chip formation for ductile polymers, and brittle fracture for brittle polymers.

Significant LEE has been reported in several wind farm projects despite the use of commercially available leading-edge protection (LEP) solutions, highlighting the fact that it is a current and key area of research for the future. Repair of wind turbine blades is reported to be costly in two ways. First, there is a degradation in the aerodynamic performance, estimated to cost the European offshore wind industry between €56 m - €75 m annually [5]. Additionally there is the need for inspection, preventative maintenance, repair, and loss of production due to down time estimated to cost the European offshore wind industry €56m annually [6]. Turbines blades, especially offshore types, are inherently difficult to access due to their size, the cost of vessel hire and environmental conditions such as weather and tidal variations [7]. As a result, removal of blades is costly and carries great risk and consequently it is used only as a last resort making *in-situ* inspection and repair the most economically viable route. In-situ repairs are limited by the need for rapid curing repair materials that can be correctly cured and applied in the environmental conditions.

A raindrop impact can be broken down into three waves: the initial longitudinal compressional stress wave, the preceding transverse shear wave, and a third Rayleigh wave due to droplet deformation from pressure rebounding from the coating (containing two thirds of the total impact energy) [3]. Failure mechanisms for rain erosion are not well understood, particularly how they are affected by elastic and viscous polymer properties at the resulting high strain rates (10^6 - 10^9 Hz) of raindrop impact [8]. These high strain rates make conventional mechanical tests and analysis unsatisfactory for studying materials erosion properties as they operate at much lower strain rates (10^1 - 10^4 Hz).

Previous studies have shown that the acoustic impedance of a material is related to its ability to resist rain erosion which can be measured using ultrasonic techniques [3]. This is a parameter that can be used in the design of coatings as a potential method for in-line monitoring during manufacture or as a key parameter that can used in a predictive model to predict erosion performance of multi-layer systems. This could allow for a method of measuring individual layers of a system after curing using a high strain rate method to predict rain erosion performance and provide data for models to determine how energy will dissipate and flow through the coating system. The theory is that how ultrasonic waves propagate through the multi-layer system is relatable to rain droplet impact waves. Currently, rain erosion performance is measured by accelerating coated samples through a simulated rain droplet environment. However, this costly method prohibits detailed evaluation of changing polymer elastic and viscous properties during testing. Kuznetsova has linked nano-particle inclusion with the acoustic impedance of a sample and this work aims to tailor individual layers (composite, filler, LEP and interfaces) to evaluate improvements in rain erosion properties [9]. Coated (Polyurethane based) glass fibre reinforced polymer (GFRP) composite samples, representative of wind turbine blades, were produced and tested.

For this study a *polyhedral oligomeric silsesquioxane* (POSS) variant was selected as the nanoparticle of choice due to its liquid state, solubility, and functionality that allows for the formation of chemical bonds between the components as opposed to just a mixture of the components.

As a prerequisite of developing an alternative ultrasonic technique, conventional tests were used to characterise commercial materials and understand the role of viscoelasticity on multi-layered systems.

2. Methodology

2.1. Materials

Unidirectional E-Glass (06-UE-591-1200) and E-Glass biaxial +/-45° (20-EX600-127) supplied by Saertex were used in combination with the RS-M135 low temperature cure epoxy resin system and hardeners (RS-MH134 and RSMH-137) supplied by PRF Composites. The commercial coating system used is comprised of a Polyurethane (PU) based filler and LEP coating. The LEP system was modified by the addition of 10 wt. % glycidyl polyhedral oligomeric silsesquioxane (POSS) cage mixture supplied by Hybrid. This POSS variant is a hybrid molecule with an inorganic silsesquioxane at the core and organic glycidyl groups attached at the corners of the cage.

2.2. Sample Manufacture

2.2.1. Flat Panels. Two 300 x 400 mm^2 ([+/-45, 0, +/-45, 0, +/-45]) composite panels were manufactured using resin infusion. The supplier's suggested mix ratio was used and infused at room temperature. The plates were simultaneously cured using the specified cure cycle (16 hours at 60 °C) with no post curing steps. The cured panels were trimmed using a diamond saw and sanded. A filler system was applied using a smoothing tool in combination with cork guides to maintain a constant thickness. Samples were then sanded followed by the application of the LEP system using a short nap roller. Two coats were applied with a wet film thickness of between 100-125 µm with a flash off time of 45 minutes.

2.2.2. Dynamic Mechanical Analysis Samples. Stand-alone filler, LEP and modified LEP (10 wt. % POSS) were cast into 100 x 150 mm^2 mould made from cork on a tool plate and allowed to cure at room temperature. Three samples of each type were machined to 35 x 10 mm^2, with approximate thicknesses of 1 mm for the filler samples and 2.9 mm for both LEP samples.

2.3. Test Methods

2.3.1. Nanoindentation. The load-hold-unload indentation cycles were conducted using a Hysitron TI Premier equipped with Berkovich shaped diamond indenters calibrated with a fused silica reference sample. Cross sections of 1 cm^2 samples were used to allow for measurement of individual layers minimising any influence from other layers detailed in Figure 1. Both load (P) and displacement (h) were continuously recorded during the experiment and a complete P- h response was obtained. As multiple indentations were made, mean values with standard deviations were reported.

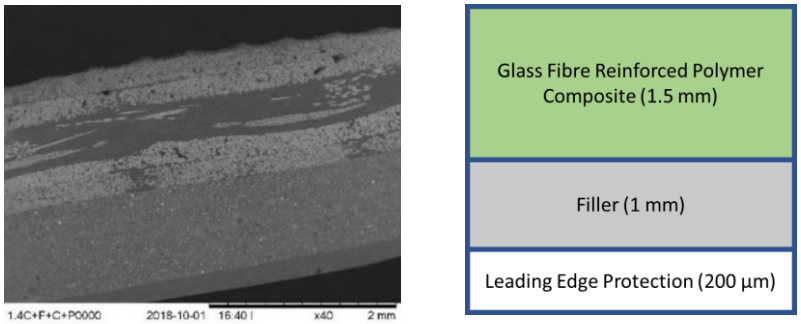

Figure 1. Cross section of test coupon. Left: SEM of sample cross section. Right: Graphic representation of cross section with approximate thicknesses.

Test 1 investigated mechanical properties of each sample layer. Testing was conducted on both the cross section and on the LEP top film surface for comparison. Loading, hold and unloading times were kept constant at 5 seconds for all indents. A series of 50 indents were made 25 nm apart in each experiment of increasing depth from 50 nm to 300 nm on each layer of the sample.

Test 2 investigated the variation of loading rate. Testing was conducted on each cross-section layer at depths of 500 nm, 700 nm, and 900 nm. A series of five indents were made 25 nm apart on each layer of the sample at loading/unloading rates of 50 nm/s, 150nm/s, and 250 nm/s with a 5 second hold time. Mechanical properties were determined from the load displacement graphs generated and summarised in Figure 2.

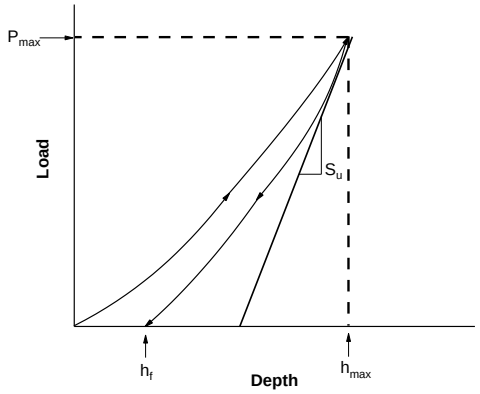

Figure 2. Example representation of indentation-load displacement data showing key parameters. P_{max}, peak indentation load, h_{max}, indenter displacement at peak load, h_f, final depth of the contact impression after unloading and S_u, contact stiffness of unloading curve calculated form the unloading gradient. Adapted from literature [10].

In this work, Oliver-Pharr analysis was used to determine the hardness and reduced elastic modulus from the unloading curve [11].

Hardness (H) is a ratio calculated by,

$$H = \frac{P_{max}}{A_c}, \tag{1}$$

where P_{max} is the maximum load and A_c is the projected area of indentation.

Unloading contact stiffness (S_u) is determined from the initial unloading slope at P_{max} by,

$$S_u = \frac{dP}{dh}, \tag{2}$$

where P and h denote the applied load and penetration depth respectively.

The reduced elastic modulus is calculated with the contact stiffness as follows,

$$E_r = \frac{S_u\sqrt{\pi}}{2\beta\sqrt{A_c}}, \tag{3}$$

where β is a factor related to the specific geometry of the Berkovich indenter.

Modulus E is determined by,

$$E = {1 - {v_s}^2} \Big/ {\frac{1}{E_r} - \left(\frac{1-{v_i}^2}{E_i}\right)}, \tag{4}$$

where E_i and V_i (1140 GPa and 0.07 respectively) represent the elastic modus and Poisson's ratio of the indenter whereas E_s and ν_s (assumed as 0.5 for PU coatings and from literature [12]) correspond to specimen values.

Short Term Recovery (STR) is a measure of elastic recovery and is thought to be a key variable in raindrop impact. This was calculated by,

$$STR = \frac{(h_{max} - h_f)}{(h_{max})}, \quad (5)$$

where h_{max} and h_f denotes maximum indenter depth and final indenter depth respectively.

2.3.2. Dynamic Mechanical Analysis. 35 x 10 mm^2 samples (filler, LEP and modified LEP) were analysed in duplicate using a TA DMA Q800 dynamic mechanical thermal analyser (DMTA) equipped with a single cantilever testing attachment. Temperature scans were conducted using a 15 µm amplitude, 1 Hz frequency and while under a dynamic scan from room temperature to 150 °C at 5 °C/min. Frequency sweeps were performed from 0.1 to 200 Hz at an amplitude of 15 µm under ambient conditions.

3. Results

3.1. Nanoindentation

Determination of mechanical properties (Test 1) was performed on both the surface and cross section of samples. Results for the unmodified LEP layer are shown in Figure 3. Samples highlighted in red were omitted from statistical analysis as they were considered as an outlier. These were defined as points which are more than 1.5 times the interquartile range (either above the third quartile or below the first quartile). This also included points indented in the first 100 nm of testing due to unreliable readings at low depths, as determination of the initial contact point of low stiffness of materials is difficult to detect [13]. Similar values for both hardness and reduced modulus were obtained but the surface indentation gave results with a much lower variation in results. This is observed in the coefficient of variation of the results with an average coefficient of variation (COV) of 31 % and 11 % for cross-section and surface indentation respectively.

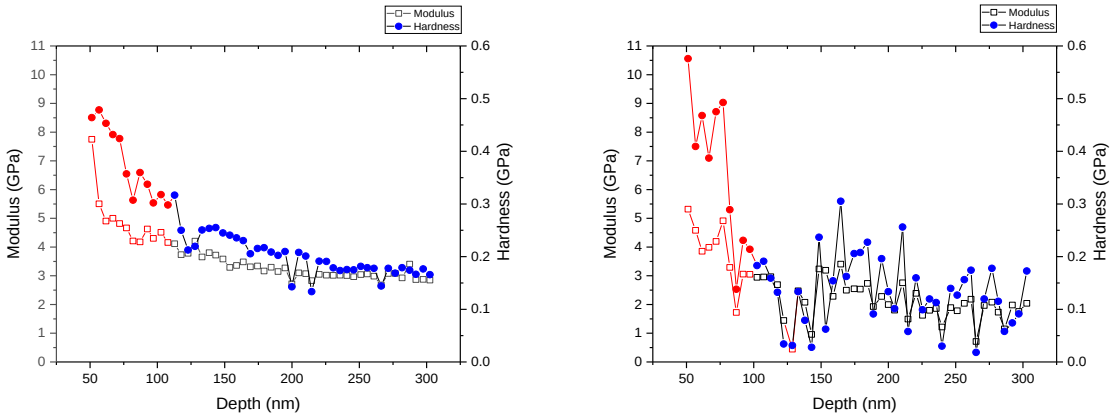

Figure 3. Nanoindentation of unmodified LEP and filler coated GFRP sample to investigate potential anisotropy. Modulus (E) and hardness (H) were determined using Oliver-Pharr analysis. Results highlighted in red are omitted from further statistical analysis. Left: Surface indentation through the LEP into the sample. Right: Indentation of cross-section of LEP film.

Contact stiffnesses and moduli for each layer cross section are summarised in Figure 4.

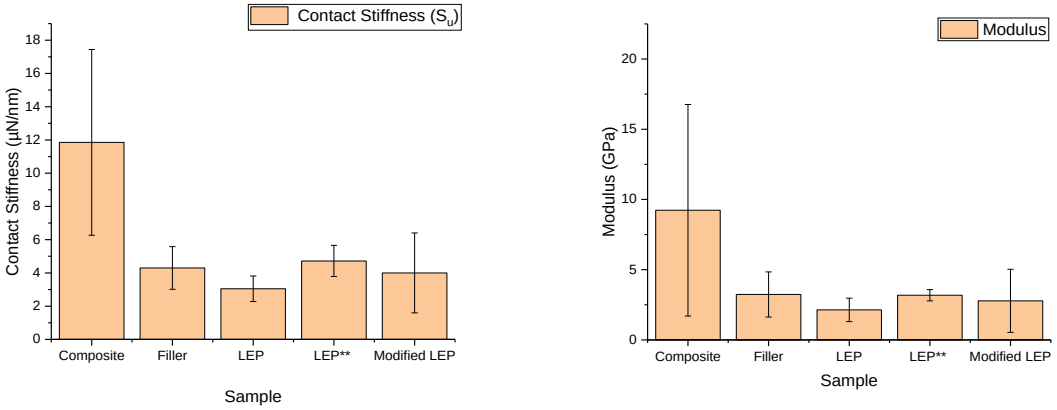

Figure 4. Nanoindentation of unmodified LEP and filler coated GFRP sample cross sections to determine mechanical properties. Contact stiffness (S_u) and modulus (E) were determined using Oliver-Pharr analysis. Contact stiffness is taken as the gradient of the unloading curve whereas modulus corrects for the compliance of the instrument in addition to assuming a Poisson's ratio of 0.5. All tests were conducted on the cross section of the sample unless denoted by ** where a surface measurement was taken. Left: Comparisons of reduced modulus. Right: Comparison of (S_u) values.

As expected, composite samples showed the highest standard deviations as they are composed of a combination of two significantly different materials (reinforcement and matrix). The modified LEP also showed high standard deviations making comparisons unviable. Statistically significant differences were seen between cross-section and surface measurements.

STR is thought to be a key parameter in rain erosion performance of materials, its correlation with loading rate could potentially be indicative of strain rates caused by varying rain impact velocities. Test 2, determination of the effect of the loading rate, was conducted on the cross section of each layer of samples and is summarised in Figure 5.

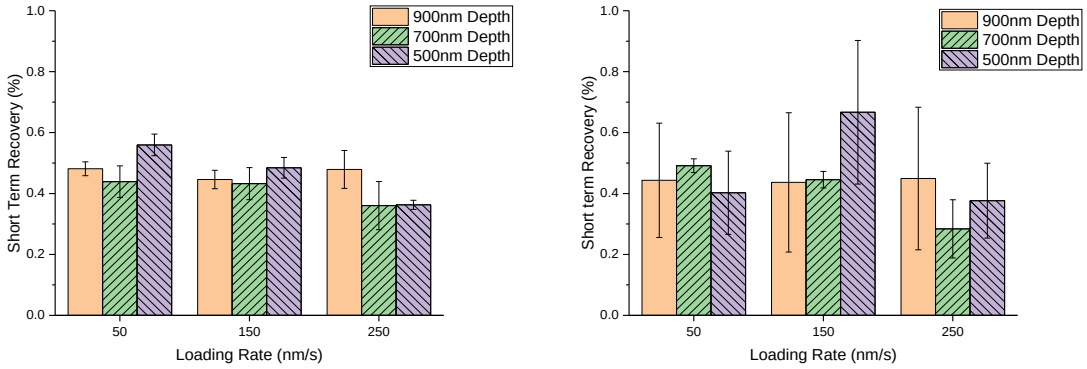

Figure 5. Nanoindentation of unmodified LEP and filler coated GFRP sample to investigate the effect of loading rate. Short term recovery was calculated from Oliver-Pharr analysis [19]. Left: Indentation of the LEP cross-section. Right: Indentation of Modified LEP (10 wt.% POSS) cross-section.

For the unmodified LEP STR at 500 nm, the increase in strain rate shows a trend of decreasing STR. The reduction in the ability of the material recover over a short period of time is thought to lead to worse rain erosion performance. This corresponds to observed increasing trends to brittle failure of coatings at increased erosion test rotational speeds. At the other indentation depths, no trend is easily observable, potentially due to insensitivity to strain rate at higher depths. As with Test 1 modified LEP results were difficult to compare, due to large standard deviations.

3.2. Dynamic Mechanical Analysis

DMTA is a technique in which a small deformation is applied to a sample in a cyclic manner allowing for the materials response to temperature, stress and frequency to be measured. A key property is the glass transition temperature (T_g), the temperature at which a polymer changes from a harder state to a more compliant or "rubbery" state. This is an important value as it could affect how materials respond to impacts at different temperatures. It is also possible to quantify the way in which a material can absorb and disperse energy using $\tan\delta$ values. It is the ratio of the loss modulus (E″), a measure of the viscous response of the material to the storage modulus (E′), a measure of the elastic behaviour of a sample. As a result, increasing the ability of a material to dissipate energy could be advantageous in minimising damage erosion caused by rain droplet impacts.
Glass transition temperature T_g values were obtained ($\tan\delta$ maximum) and onsets calculated from the storage modulus plot in Figure 6. The unmodified filler showed a lower T_g (54 °C) and lower storage modulus between 40 - 80 °C in comparison to the LEP samples. The unmodified filler also indicated that the storage modulus begins to decrease at temperatures lower than 30 °C. No significant difference between T_g values (85 °C) of LEP samples was observed however modified LEP showed a higher $\tan\delta$ value between 30 – 80 °C. This shows an increase the ability of a material to dissipate energy which could be advantageous in minimising damage erosion caused by rain droplet impacts.

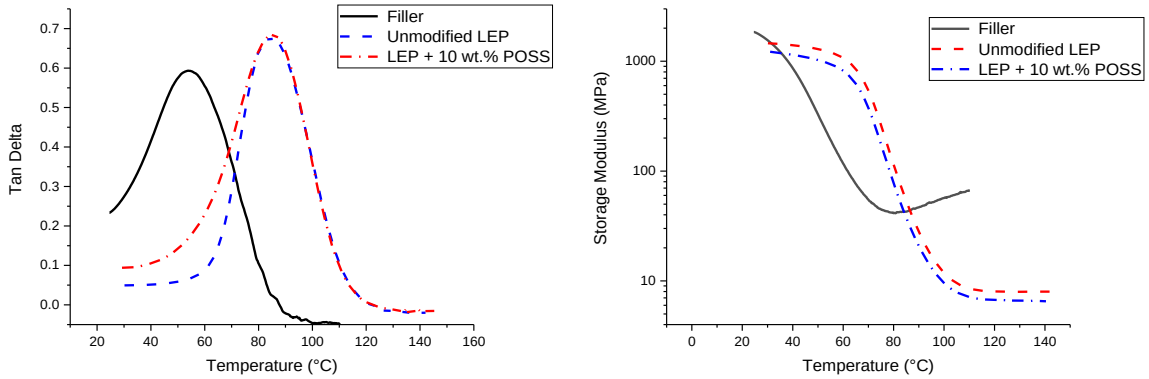

Figure 6. Comparison of filler, unmodified LEP and modified LEP (10 wt. % POSS) DMTA single cantilever temperature scans conducted using a 15 μm amplitude, 1 Hz frequency and while under a dynamic scan from room temperature to 150 °C at 5 °C/min. Left: $\tan\delta$ comparison. Right: Storage modulus comparison.

Frequency sweep data displayed that the unmodified filler $\tan\delta$ value varies greatly in comparison to the two LEP systems showing a much greater decrease over the frequency range (Figure 7). Both LEP samples showed similar trends in $\tan\delta$ values with little variation from low to high frequencies, but modified LEP consistently had a higher value at all frequencies measured, indicating improved energy dissipation. Storage modulus of both LEP samples varied accordingly (loss to storage ratio relationship) and showed similar trends of following a slight increase in storage modulus until stabilising. However,

the unmodified LEP showed higher storage modulus values of approximately 300 MPa at all frequencies. The filler storage modulus also increased above both LEP samples.

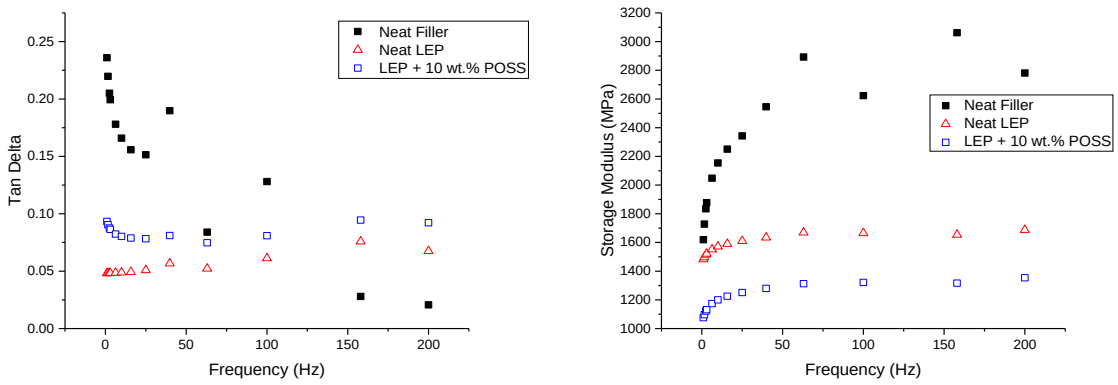

Figure 7. Comparison of filler, unmodified LEP and modified LEP (10 wt.% POSS) DMTA single cantilever frequency sweeps conducted under 0.1 to 200 Hz at an amplitude of 15 µm under ambient conditions. Left: tan δ comparison. Right: Storage modulus comparison.

4. Discussions

4.1. Nanoindentation

The use of nanoindentation offers a relatively fast, repeatable and non-destructive technique for evaluating mechanical properties of solid materials [10, 14]. Although initially used for metallic materials, its use in polymer characterisation has become more common. For the measurements to be representative of the bulk properties, homogeneity of the micro structure is required [14].

The difference between surface and cross section results could indicate either the general rule of omitting readings below 10% the total layer thickness to avoid substrate influence does not apply to this material. Alternatively, there is anisotropy of the material potentially induced during manufacturing. As the LEP cures upon reaction with ambient moisture, the surface and inner properties may differ due to a gradient of different degrees of cure. This effect could be minimised by only comparing results from the same depth.

Traditionally the dispersion of nanoparticles in polymeric materials has been problematic and commonly results in phase separation or agglomeration. The addition of nanoparticles can cause the system to become heterogenous and can explain the increase in variation seen in modified LEP samples. An example of this can be seen in studies using nanoindentation with concrete as a result of its heterogeneous nature. Studies require a large series of indentation tests (100+) to reach convergence of mechanical properties with an error of less than 5%.

Moduli were reported through the study but the Poisson's ratio of the LEP was not obtained during this study and was assumed from literature. As a result, there was no difference in value used between both LEP samples which potentially could be incorrect as the addition of crosslinks will alter the material properties, especially at high POSS concentrations. Previous work has also highlighted that the Poisson's ratio of PU varies depending on the strength of impact varying between 0.39 for weak impacts and 0.5 for increased impact strength which was not accounted for in this study [12]. This parameter could be of importance to tune rain erosion properties.

Varying loading rate showed limited trends due to large error bars, especially in the modified LEP samples. However, a correlation between increased loading rate and a decrease in STR was observed. Although not directly comparable, loading rate could be compared with strain rate seen from increasing the rotational speed of a specimen. According to literature higher tip speeds are a key factor in defining the severity of rain droplet impacts and as a result LEE damage [15]. This can be explained by the increase in kinetic energy E_K of the droplet:

$$E_K = \frac{1}{2}mv^2$$

where m is the mass of the droplet and v is the velocity of the particle relative to the blade surface (considered equivalent to blade speed). As a result of the square relationship it can be seen that velocity is the more important factor.

During testing it was observed from the load-displacement curves that stress relaxation was occurring during the hold phase of the test *i.e.* a decreased stress response to the same amount of strain generated in the structure. This can be linked to the viscous response of polymer as they behave in a non-linear and non-Hookean manner. Addition of reinforcements to a system generally slows the relaxation effect. This suggests that any increase in crosslinking, which hinders molecular flow of the polymer near the interface, could be used to tailor this property. However, the effect of this on rain erosion properties need to be further tested. It could be assumed that increasing the stress relaxation of the coating would improve energy dissipation and potentially minimise the effects from the combination of subsequent impacts preventing initiation of damage.

4.2. Dynamic Mechanical Thermal Analysis

The addition of nanoparticles is expected to diminish the intensity of the $\tan\delta$ response. This is due to the hinderance of molecular motion of the polymer chains, resulting in an increase in the elastic response of the material and a reduction in the viscous response. There is a reduction in the $\tan\delta$ intensity below 80 °C indicating an increase in elasticity. This could be further explored by the variation of POSS loadings and using localised spectral analysis to quantify dispersion.

The filler displayed a lower T_g value than that of the two LEP systems, with a reduction of the storage modulus observed at the lowest measured temperature of 30 °C. At these temperatures the filler which acts as an interfacial layer between the substrate and LEP coating can begin to lose elasticity near rain erosion test temperatures. The $\tan\delta$ response shows that modification of the LEP increases damping at lower temperature ranges introducing an additional mechanism of dissipating energy, which could potentially be of benefit to rain erosion performance. This is potentially of interest as it raises questions about test methods that utilise closed vessels. This is supported by thermocouple measurements in a rain erosion test rig which show tests conducted at room temperature can see a 4 °C temperature rise over 20 minutes of testing. This is due to air friction and localised heat generated from the high strain rain impacts, which could reduce the filler elasticity as testing progresses. However, in turbine blades the temperatures are expected to be much lower due to steady state temperature of the environment which necessitates further analysis at lower temperatures.

Frequency sweeps were utilised to investigate higher strains rates occurring during both increased rotational speed (higher tip speeds) and in increasing droplet size due to the increased penetration depth imparted onto the surface upon impact. The data showed that at increasing strain rates, the filler storage modulus increases significantly resulting in an increase in its elasticity and decrease in the viscous response. The Unmodified LEP showed an increase in $\tan\delta$ as frequency was increased. Modified LEP samples displayed lower $\tan\delta$ values at all frequencies, with an initial decrease followed by increase in $\tan\delta$ upon increasing frequency. This shows that the elasticity of the coating system increases with frequency of deformation which would result in less energy being dissipated after a rain impact.

5. Conclusions

This work obtained previously unreported mechanical properties for this commercial PU based coating system (hardness, modulus, and short-term recovery). Results show that the inclusion of POSS improves damping, providing an alternative mechanism for energy dissipation without variation of T_g and minimal loss of stiffness. This presents a way of modifying current coating systems through the incorporation of POSS.

The investigation into varying strain rate at the lowest measured depth showed a correlation between increased loading rate and a reduction in STR, which could be linked to increased rotational speeds in erosion testing. Generally, nanoindentation was difficult for modified samples as it resulted in large standard deviations. A potential reason discussed was the poor dispersion of POSS throughout the samples. The difference between results measured from the sample cross section and surface suggested potential anisotropy, a phenomenon seen already in PU foams [16]. DMTA was used to characterise the individual components of the coating system (both unmodified and modified with POSS) and identified differences between components in terms of frequency and temperature dependency. It is not clear if matching or mismatching these properties aids rain erosion performance. Testing also highlighted the low T_g of the filler which begins to lose its elasticity at low temperatures in comparison to the LEP. This could be a potential issue in closed test environments where operating temperatures can rise due to testing, especially as it is the interface between the outer coating layer and the composite substrate. Generally, results have been supported by preliminary rain erosion test results to be published in future work.

6. References

[1] Kay A. *Blade Leading Edge Erosion Programme (BLEEP): Reducing the Cost Impacts of Wind Turbine Blade Erosion*. Glasgow, 2016.
[2] Chen J, Wang J, Ni A. A review on rain erosion protection of wind turbine blades. *J Coatings Technol Res* 2018; 1–10.
[3] Cortés E, Sánchez F, O'Carroll A, Madramany B, Hardiman M, Young TM. On the Material Characterisation of Wind Turbine Blade Coatings: The Effect of Interphase Coating-Laminate Adhesion on Rain Erosion Performance. *Mater (Basel, Switzerland)* 2017; 10: 1146–1168.
[4] Dalili N, Edrisy A, Carriveau R. A review of surface engineering issues critical to wind turbine performance. *Renew Sustain Energy Rev* 2009; 13: 428–438.
[5] Wiser RH, Jenni K, Seel J, Baker E, Hand MM, Lantz E, Smith A. *Forecasting Wind Energy Costs and Cost Drivers: The Views of the World's Leading Experts*. 2016. Epub ahead of print 2016. DOI: 10.1016/S0379-6779(99)00311-2.
[6] Herring R. Integration of Thermoplastic/Metallic Erosion Shields into Wind Turbine Blades to Combat Leading Edge Erosion. In: *Fraunhofer Offshore Wind R&D 2018*. Bremerhaven, Germany, 2018.
[7] Keegan MH. *Wind Turbine Blade Leading Edge Erosion: An investigation of rain droplet and hailstone impact induced damage mechanisms*. 2014.
[8] Dyer K. Developing Tools to Improve Leading Edge Erosion Coatings. In: *Wind Blade Materials Development Forum*. Hamburg, Germany: TBM, 2018.
[9] Kuznetsova IEE, Zaĭtsev BD, Shikhabudinov AMM, Zaĭtsev BD, Shikhabudinov AMM. Effect of the nanoparticle material density on acoustic parameters of polymer-based nanocomposites. *Tech Phys Lett* 2010; 36: 759–761.
[10] Hainsworth S V., Chandler HW, Page TF. Analysis of nanoindentation load-displacement loading curves. *J Mater Res* 1996; 11: 1987–1995.
[11] Pharr GM. An improved technique for determining hardness and elastic modulus using load and displacement sensing indentation experiments. *J Mater Res* 1992; 7: 1564–1583.
[12] Tsukinovsky D, Zaretsky E, Rutkevich I. Material behavior in plane polyurethane-polyurethane impact with velocities from 10 to 400 m/sec. *J Phys IV JP* 1997; 7: 335–339.
[13] Guillonneau G, Kermouche G, Bec S, Loubet J-L. Determination of mechanical properties by nanoindentation independently of indentation depth measurement. *J Mater Res* 2012; 27: 2551–2560.
[14] Voyiadjis GZ, Samadi-Dooki A, Malekmotiei L. Nanoindentation of high performance semicrystalline polymers: A case study on PEEK. *Polym Test* 2017; 61: 57–64.
[15] MacDonald H, Infield D, Nash DH, Stack MM. Mapping hail meteorological observations for prediction of erosion in wind turbines. *Wind Energy* 2016; 19: 777–784.

[16] Huber AT, Gibson LJ. Anisotropy of foams. *J Mater Sci* 1988; 23: 3031–3040.

Acknowledgments
This work was supported by the Engineering and Physical Sciences Research Council through the EPSRC Centre for Doctoral Training at the Advance Composites Centre for Innovation and Science (ACCIS, Grant number EP/L016028/1), and The Future Composites Manufacturing Hub (Grant number EP/P006701/1). This project was also funded by the Wind Blades Research Hub (WBRH), a joint collaboration between the University of Bristol and ORE Catapult. The author would also like to acknowledge Cainan Long and Cameron Mackie for help with testing.